

Cepheid Distance to M100 in Virgo Cluster

D. Narasimha¹ and Anwesh Mazumdar²

Department of Astronomy and Astrophysics, Tata Institute of Fundamental Research,
Homi Bhabha Road, Mumbai 400005, India.

ABSTRACT

A measurement of the distance to Virgo Cluster by a direct method along with a realistic error analysis is important for a reliable determination of the value of Hubble Constant. Cepheid variables in the face-on spiral M100 in the Virgo Cluster were observed with the Hubble Space Telescope in 1994 under the HST Key Project on the Extragalactic Distance Scale. This work is a reanalysis of the HST data following our study of the Galactic Cepheids (in an accompanying communication). The periods of the Cepheids are determined using two independent methods and the reasons for varying estimates are analyzed. The $\log(\text{period})$ vs V -magnitude relation is re-calibrated using LMC data as well as available HST observations for three galaxies and the slope is found to be -3.45 ± 0.15 . A prescription to compute correction for the flux-limited incompleteness of the sample is given and a correction of 0 to 0.28 magnitude in V -magnitude for Cepheids in the period range of 35 to 45 days is applied. The extinction correction is carried out using *period vs mean $(V - I)$ color* and *V -amplitude vs $(V - I)$ color at the brightest phase* relations. The distance to M100 is estimated to be 20.4 ± 1.7 (random) ± 2.4 (systematic) Mpc.

Subject headings: Cepheids — distance scale — galaxies: individual (M100)

1. Introduction

A natural scale length for the Universe is provided by the Hubble Constant (H_0) and undoubtedly a determination of its value is one of the fundamental problems of cosmology. Over the years, there has been much debate about the value of H_0 and the present

¹e-mail: dna@astro.tifr.res.in

²e-mail: anwesh@astro.tifr.res.in

estimates range from less than $50 \text{ km s}^{-1} \text{ Mpc}^{-1}$ to over $80 \text{ km s}^{-1} \text{ Mpc}^{-1}$. Most probably the major reason for the discrepancy is the conventional distance ladder involving multiple steps. Its main drawback is that analysis of the systematic errors becomes difficult when the calibrating local sample and the observed sample at the next step of the ladder are not identical. Consequently, it is believed that an accurate measurement of the distance to a galaxy cluster which is $\sim 20\text{--}30 \text{ Mpc}$ away, without involving intermediate steps, will lead to a reliable direct estimate of the value of H_0 , provided the recession velocity of the cluster is independently known. The Virgo Cluster, which is our nearest cluster of galaxies, is fairly rich in terms of galaxy population, and an average of the distances to the individual galaxies by different methods would provide a good estimate to its mean distance.

One of the key projects of the Hubble Space Telescope (HST) was devoted to the calibration of the extragalactic distance scale for a determination of H_0 with reasonable accuracy. An examination of the systematic errors in the Cepheid period–luminosity relation and measurement of the distance to the Virgo Cluster through Cepheid observation were among the primary aims of this key project. The nearly face-on spiral M100 in the Virgo Cluster was observed on 12 epochs over a span of ~ 57 days in 1994 with the HST using the filters F555W and F814W, which are almost equivalent to the Johnson V and Cousins I bands respectively (Freedman et al. 1994). The advantage of choosing this particular galaxy is that being nearly face-on, the errors due to extinction and reddening are expected to be minimal, and further, it is considered to be very similar to the Milky Way in terms of age, chemical composition etc. However, its position relative to the center of the Virgo Cluster is not known accurately, and that introduces some uncertainty in the Virgo distance derived from direct distance estimation to M100. Ferrarese et al. (1996) reported observations of 70 Cepheids in M100, and obtained a distance of $16.1 \pm 1.3 \text{ Mpc}$. The value of the Hubble Constant was calculated to be $88 \pm 24 \text{ km s}^{-1} \text{ Mpc}^{-1}$. On the other hand, Sandage and collaborators re-calibrated the distance to a few galaxies, where supernovae of type Ia were detected earlier, by observing the Cepheids in those galaxies with the HST. They obtained a mean absolute B magnitude at peak of -19.6 for normal SN Ia and consequently, a value of $52 \pm 9 \text{ km s}^{-1} \text{ Mpc}^{-1}$ for the Hubble Constant (Sandage et al. 1994; Saha et al. 1994). However, more recent publications indicate a better reconciliation in the value of H_0 . Freedman et al. (1998) summarize a value of 73 ± 6 (statistical) ± 8 (systematic) $\text{km s}^{-1} \text{ Mpc}^{-1}$, as compared to 55 ± 3 (internal) $\text{km s}^{-1} \text{ Mpc}^{-1}$ quoted by Sandage’s group (Saha et al. 1996).

The present work is a re-analysis of the HST data on M100 Cepheids, based on a general calibration of Galactic Cepheids, presented in a companion paper (which we refer henceforth as Paper I). The specific problems we address here are the following:

- Period–Luminosity relation applicable to the Cepheids of period $\gtrsim 15$ days generally

observed in distant galaxies.

- Importance of the incompleteness correction and quantification of the effect.
- Uncertainty in the periods of the Cepheids in M100 due to the phase sampling techniques applied as well as the large error in V -magnitude, particularly at low flux levels.

The central idea behind distance measurement with Cepheids is the period–luminosity relation. However, the values of both the slope and the intercept of this relation continue to be subjects of lively debate. There appears to be a distinct difference in the value of the slope between Cepheids of low and high periods. While applying the period–luminosity relation to distant galaxy samples, where only higher period Cepheids can be detected due to flux limitation, this distinction becomes even more crucial. We address this question on the basis of our study of Galactic Cepheids (Paper I) which demonstrates a clear division between two classes of Cepheids, one with periods ≤ 15 days, the other at higher periods. The zero-point of the period–luminosity relation is another quantity which needs to be fixed unambiguously in order to obtain reliable estimates of distance. We use the recent calibration of the local Cepheids by the Hipparcos mission (Feast & Catchpole 1997), rather than the distance to the Large Magellanic Cloud which is normally treated as the calibrating point for the distance scale.

A crucial aspect of our new analysis is the correction for incompleteness of the Cepheid sample. Since the Cepheid period–luminosity relation has an intrinsic scatter due to the finite width of the instability strip at a given period, the Cepheids are observed to be spread over a range of luminosities. All the observed Cepheids in M100 have V -magnitudes between 24 and 27 mag. At such faint flux levels it is very likely that for a fixed period, the fainter Cepheids would escape detection, and only the brighter ones will appear in the surveys. This selection bias would have a systematic effect on the period– V -magnitude slope, especially at low periods, reminiscent of the Malmquist bias discussed in the literature. In order to counter this effect, one has to take into account the undetected Cepheids, which can be done by adequately correcting the observed magnitudes to fainter levels. Obviously, the amount of correction depends on the scatter of the period–luminosity diagram. We have devised a formalism to correct for this incompleteness effect which we demonstrate to be present to a large extent in the M100 sample.

We have tried to estimate the correction for extinction and reddening, which again, is based on our study of Galactic Cepheids (Paper I). However, in the absence of multi-wavelength observations, this treatment is rather limited, and is based on period–color–amplitude relations of Cepheids. Also, for the same reason we could not isolate the extinction correction from the incompleteness correction which ideally we should have been able to.

This paper is organized as follows. In Section 2 we present our methods of determination of Cepheid periods and photometric parameters. The question of choosing the correct period–luminosity relation is addressed in Section 3. In Section 4, we devise a formalism for the incompleteness correction of a biased Cepheid sample, and the mathematical aspects of compensation for flux-limited bias are described in the Appendix. Section 5 deals with the reddening and extinction corrections and the essentials of the numerical methods. The results and major contributions to errors are discussed in Section 6 and some remarks on the conclusions are presented in Section 7.

2. Determination of Period, Color and Magnitude

Ferrarese et al. (1996) have tabulated the observed periods as well as magnitudes after conversion to an equivalent V and I band for the 70 Cepheids in M100 observed by the HST in 1994. For each Cepheid, there are at most 12 V and 4 I band data, very often only 11 in V and 3 in I band that are useful for the analysis. We estimate from an inspection of the HST data, that the signal to noise ratio for the F555W filter (V-band) data is typically 6 to 8 for low period Cepheid variables and 10 to 15 for the higher period ones. The signal to noise ratio for the F814W filter is in general worse, but the data turns out to be useful when we have to discriminate between two independent estimates of the period computed from the V-band data.

A determination of the period and amplitude from sparsely sampled data with inadequate signal to noise ratio does not generally yield a unique result. According to Bhat, Gandhi and Narasimha (1998), a reasonable criterion to obtain the period approximately 98% of the times to better than 2% accuracy may be stated as follows: If the signal to noise ratio (SNR) is better than 30 and there are two independent sine components in the signal, 13 optimally spaced sampling points are sufficient to extract the signal, but if there are three components we require 15 data points. For SNR decreasing from around 30 to 10, the requirement increases approximately linearly with the inverse of SNR from 15 to 22 samplings for a three-component signal and thereafter the requirement appear to increase more rapidly to 36 data points when SNR is 3. Naturally, the HST data on M100 could yield somewhat differing periods and amplitude of pulsation depending on the method employed. We decided to recompute the periods by two independent methods for comparison with the periods given by Ferrarese et al. (1996).

We used a modified version of the period-searching program by Horne and Baliunas (1986) based on the method due to Press and Rybicki (1989). When our derived periods were substantially different from the value obtained by the HST Group, we used a template

for the V and I band light curves prepared on the basis of the Galactic Cepheid variables (cf. Paper I) to get another estimation for the pulsation period. Our final periods agree with those of Ferrarese et al. to within 10% in general, but at high periods, in some cases the discrepancy is higher. We present a comparison of the light curves of a typical M100 Cepheid, C38 obtained by us with the one derived by the HST group in Figure 1.

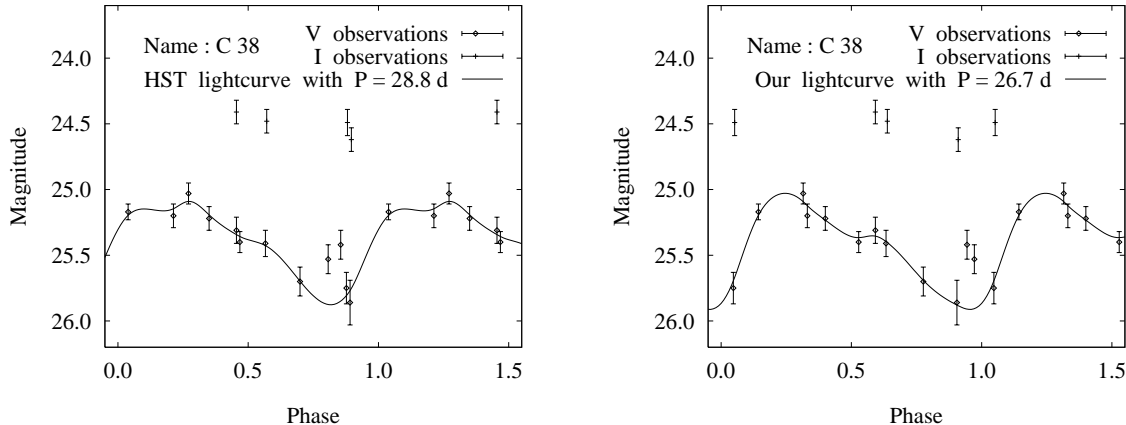


Fig. 1.— Light curves constructed for the same Cepheid with different periods are compared. Our light curve with $P = 26^{\text{d}}.7$ resembling a characteristic Cepheid light curve, has a better phase matching for the I data than the HST light curve with $P = 28^{\text{d}}.8$.

From the plot of the number density of Cepheids against $\log(P)$ (Figure 2) we note that there is a dip in the number density in the range $1.5 \leq \log(P) \leq 1.65$. In our view, this is caused owing to the lack of identification of a source as a Cepheid, a problem which becomes particularly severe while observing at fixed epochs over a finite length of time which is comparable to the Cepheid period. According to Saha and Hoessel (1990) in order to obtain a minimal light curve, it is essential to have enough number of observations near both light maximum and light minimum phases during a cycle. By observing at predetermined 11 or 12 epochs one would invariably fail to detect the variation of light of a source within a certain range of periods at crucial points in its light curve, and such a source could be easily missed as a variable source. Indeed, such a dip is predicted from the observing strategy by Ferrarese et al. (1996) also.

We determined the V magnitudes by integration of the light curves. We used the method of synthetic light curves (cf. Paper I) to obtain $\langle V - I \rangle$. Out of the 70 stars listed in Ferrarese et al. (1996), ten have been excluded: three of them due to their low period; two because we believe that their period is much larger than the total time span of observation (56 days) and consequently, the width of their plateau in the light curve near minimum flux cannot

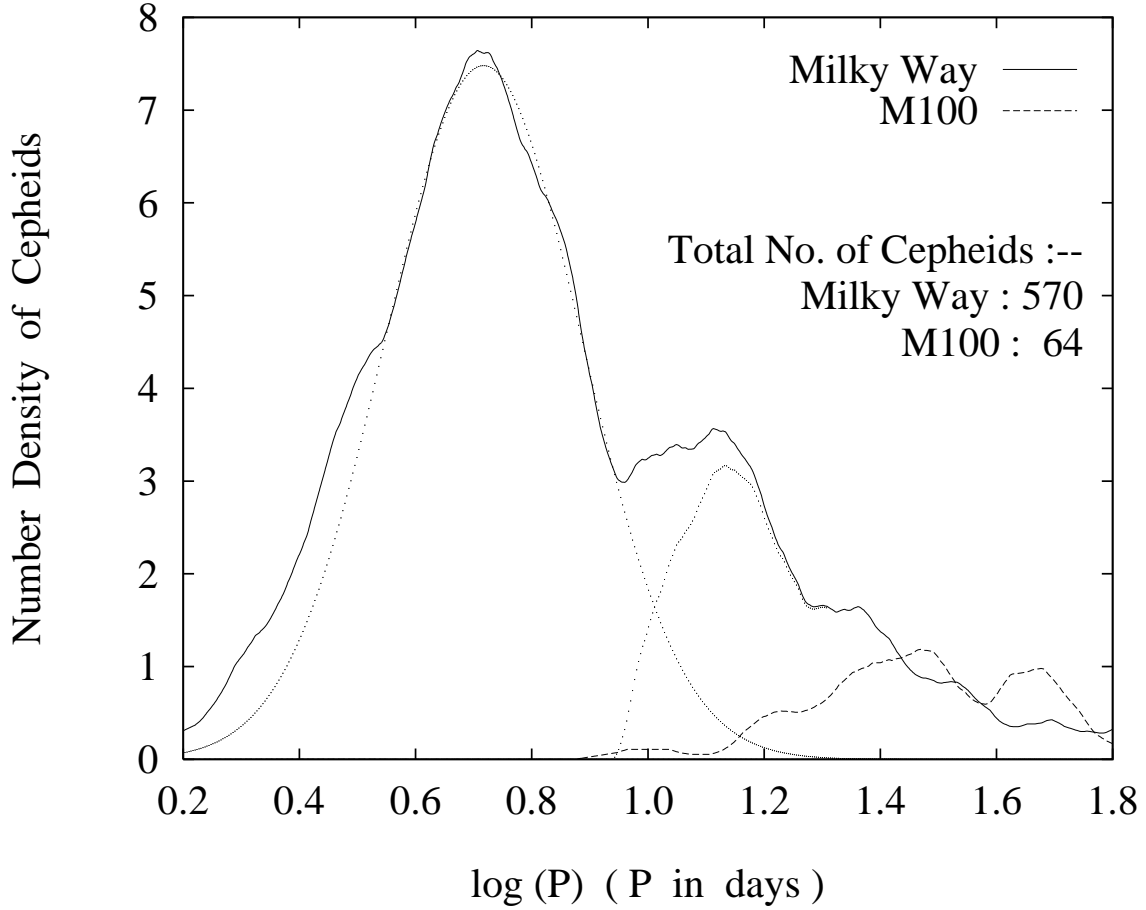


Fig. 2.— The number density distribution against $\log(P)$ is shown for Cepheids in the Milky Way and M100. A moving average has been used to generate a smooth curve from discrete observations. The Galactic sample is split into two populations, having slight overlap between periods of 9 and 18 days. The M100 sample lies almost fully in the second population with $P \geq 9$ days.

be determined; four stars for which the light curve does not appear to conform to Cepheid variables for any of the converged periods within the allowed range; one which had only one I band data. Our final working sample consists of 60 Cepheid variables with a period range of 15 to 69 days. A comparison of our derived periods with those obtained by the HST Group is shown in Table 1 where we have also given the mean V -magnitude ($\langle V \rangle$), $\langle V - I \rangle$ color, amplitude of pulsation (ΔV) as well as the extinction-corrected V -magnitude ($\langle V \rangle_0$) that we have estimated.

Table 1. M100 Cepheid parameters

ID	Period (in days)		Photometric magnitudes from light curves				
	Ferrarese ^a	This work	$\langle V \rangle$	ΔV	$\langle V - I \rangle$	$(V - I) _{\text{at } V_{\text{max}}}$	$\langle V \rangle_0$
C1	85.0
C2	66.2	69.0	25.159	0.445	1.296	1.254	24.264
C3	62.1
C4	54.0	55.2	25.224	0.857	1.235	1.074	24.446
C5	53.4	52.2	25.035	0.655	1.075	0.947	24.640
C6	52.0	45.9	25.221	0.834	0.689	0.674	25.221
C7	50.6	56.0	24.758	0.671	0.891	0.868	24.758
C8	50.2	51.0	24.981	0.439	0.939	0.881	24.839
C9	50.1	48.0	25.886	0.597	0.989	0.947	25.522
C10	50.0	48.0	24.702	0.674	0.899	0.766	24.702
C11	48.0	51.5	25.492	0.828	1.127	0.913	24.953
C12	47.9	50.0	25.304	0.778	1.323	1.063	24.435
C13	47.0	47.5	25.483	0.612	1.121	0.911	24.963
C14	46.0	48.0	24.945	0.806	1.023	0.854	24.667
C15	43.8	42.5	25.438	0.853	1.075	0.864	24.999
C16	41.8	42.0	24.908	0.634	1.086	0.929	24.471
C17	41.7	42.3	24.982	0.804	1.139	1.138	24.982
C18	42.0	43.0	25.211	0.958	0.937	0.743	25.050
C19	36.4	32.3	25.749	0.787	0.901	0.616	25.749
C20	41.6
C21	40.7	42.0	25.324	0.787	0.948	0.889	25.068
C22	41.5	41.2	25.439	0.687	0.589	0.540	25.439
C23	39.7	40.5	25.640	0.657	1.101	0.904	25.106
C24	36.4	33.5	25.670	0.915	0.843	0.504	25.670
C25	35.1	31.0	25.853	0.392	0.628	0.510	25.853
C26	34.1	42.0	25.885	0.779	1.253	1.123	24.997
C27	34.1	35.1	26.151	1.137	1.036	0.764	25.709
C28	33.1	31.3	25.611	0.353	0.834	0.833	25.611
C29	33.0
C30	32.4
C31	30.9	32.6	25.499	0.672	0.741	0.695	25.499
C32	30.9	31.0	26.067	1.197	0.760	0.304	26.067
C33	31.6	31.6	25.766	1.412	0.961	0.743	25.378
C34	30.4	24.5	26.132	1.308	0.802	0.343	26.132
C35	29.8	29.5	26.171	1.090	1.286	1.087	25.061
C36	29.7	29.2	25.417	0.675	0.618	0.487	25.417

Table 1—Continued

ID	Period (in days)		Photometric magnitudes from light curves				
	Ferrarese ^a	This work	$\langle V \rangle$	ΔV	$\langle V - I \rangle$	$(V - I) _{\text{at } V_{\text{max}}}$	$\langle V \rangle_0$
C37	28.9	30.1	26.180	1.015	1.219	1.123	25.236
C38	28.8	26.7	25.395	0.721	0.915	0.744	25.346
C39	28.5	29.7	26.162	1.026	1.190	0.902	25.371
C40	28.9	31.0	26.069	0.786	0.996	0.966	25.559
C41	27.2	27.9	24.896	0.633	0.784	0.746	24.896
C42	26.1	26.0	25.855	1.069	0.976	0.767	25.494
C43	24.4	26.0	25.539	0.928	0.520	0.468	25.539
C44	25.7
C45	25.8	25.8	25.672	1.080	1.008	0.820	25.223
C46	26.0	25.4	25.336	0.966	0.548	0.332	25.336
C47	25.6	29.0	26.153	0.711	1.055	0.885	25.604
C48	24.7	24.4	25.961	1.071	1.029	0.682	25.671
C49	24.4	24.2	26.300	1.243	1.093	0.749	25.683
C50	25.0	23.4	26.182	1.476	1.069	0.551	25.570
C51	23.9	24.3	25.976	1.201	1.009	0.683	25.676
C52	23.4	21.4	26.575	0.949	0.804	0.458	26.575
C53	21.9	22.5	26.521	1.216	0.941	0.816	26.050
C54	21.3	21.4	26.219	1.281	1.088	0.530	25.548
C55	22.5	19.5	26.474	0.851	1.118	0.823	25.869
C56	21.3	21.0	26.250	1.858	0.766	0.372	26.250
C57	20.2	21.4	26.436	0.560	1.246	1.065	25.592
C58	19.9	19.7	25.733	1.050	0.587	0.447	25.733
C59	19.0	22.5	25.491	0.960	0.619	0.555	25.491
C60	17.1	17.5	26.174	0.855	1.184	1.027	25.337
C61	18.4
C62	17.9	17.3	26.100	1.374	0.961	0.567	25.788
C63	17.6	17.0	26.092	1.213	1.193	0.843	26.092
C64	17.1	16.5	25.803	0.787	0.510	0.484	25.803
C65	15.2	15.7	25.937	0.729	0.529	0.357	25.937
C66	15.7	15.8	26.280	1.121	0.451	0.154	26.280
C67	14.1	14.6	26.458	0.774	1.315	1.308	26.458
C68	10.9	10.9
C69	9.2	9.2
C70	7.3	7.3

^aFrom Ferrarese et al. (1996)

One major handicap of our analysis is the uncertainty in the determination of $\langle V - I \rangle$ in many cases; this is caused by the extremely poor phase sampling in the I band. In general, for reliable period determination, better phase coverage in at least one band, effected by either larger number of observations, or better choice of sampling phase points, is essential. As we shall see later, the uncertainty in the period determination translates to an increased scatter in the period–luminosity diagram and leads to a substantial increase in the error margin in the distance measurement.

3. Period–Luminosity Diagram for the Classical Cepheids

The slope and intercept of the period–luminosity diagram is conventionally derived by using the LMC Cepheids in the period range of 3 to 60 days and the value of the slope is usually taken as -2.77 . However, as argued in Paper I, at low periods, many of the classical Cepheid variables are multi-mode pulsators and most often the first or second overtone is the dominant mode of pulsation. But at higher periods, by and large, the fundamental mode appears to be important. It has been established in Paper I that we may split the parent Cepheid population into two broad groups, according to their pulsation characteristics. For galaxies at far off distances, only the Cepheids with high luminosity (i.e., those with higher periods, and probably with dominant fundamental mode of pulsation) are detected. A comparison of the number densities of Cepheids at different periods in the Milky Way and M100 (Figure 2) clearly shows the two broad groups detected among Galactic Cepheids, signified by the two peaks at periods around 7 and 16 days; on the other hand, in the M100 population, only the second group is detected, while the low-period Cepheids are missed due to flux limitation. The slope of the period–luminosity relation derived by using all Cepheids is heavily biased towards the low-period ones because of their numerical strength in our neighborhood. So a calibration of the period–luminosity relation which is relevant for distant galaxies should be made in nearby galaxies *only with Cepheids of period greater than 15 days*, avoiding contamination from low-period pulsators, which have, on the average, a different slope in the period–luminosity relation.

We have calibrated the slope of the period– V magnitude diagram by selecting only the Cepheids in the period range of 15 to 70 days in LMC as well as three spirals at moderate distances for which HST data is available. To the extent possible from the available data, we have tried to do it with extinction correction, as well as without; but since extinction correction does not affect the slope of a complete sample, we have displayed the typical numbers in Table 2 without extinction correction. It is readily seen from this table that there is a systematic change in the slope with increasing period ranges but within the range

of 20 to 60 days it remains fairly constant. This effect was recognized earlier by Morgan (1994) who had noted that a better fit to the period–luminosity diagram is obtained if the slope for higher period Cepheids is taken as -3.54 . From a general study of all these four galaxies, we arrive at an average slope of -3.45 for Cepheids between periods of 15 and 70 days, with a possible error of 0.15.

Table 2: Slope of the Cepheid Period-Luminosity Relation from different galaxies

Galaxy	Period range	No. of Cepheids	Slope of PL relation	$\sqrt{\chi^2/\text{d.o.f}}$	Source of the data
LMC	all	108	-2.770	0.360	Freedman (1995)
	$\log(P) \geq 1.16$	35	-3.405	0.335	
	$\log(P) \geq 1.20$	34	-3.445	0.340	
	$\log(P) \geq 1.26$	30	-3.480	0.325	
	$\log(P) \geq 1.30$	28	-3.526	0.336	
NGC 925	$\log(P) \geq 1.27$	30	-3.615	0.294	Silbermann et al. (1996)
	$\log(P) \geq 1.31$	28	-3.493	0.291	
	$\log(P) \geq 1.35$	24	-3.447	0.297	
IC 4182	$\log(P) \geq 1.12$	12	-3.394	0.269	Saha et al. (1994)
NGC 3351	$\log(P) \geq 1.00$	32	-3.390	0.283	Graham et al. (1997)
Our accepted value	$\log(P) \geq 1.15$		-3.450 ± 0.15		

Just as the slope of the period– V -magnitude relation needs to be determined for the representative sample of Cepheid variables, it is equally important to find the scatter in the relation if we intend to provide a trustworthy error analysis of our distance estimations. The data we have used cannot provide a good estimate for the scatter in the extinction corrected period– V -magnitude relation for Cepheids of period in the range of 15 to 70 days which are in their second passage of the instability strip. A value of 0.20 to 0.25 magnitude appears to be indicated by our analysis of the HST data for some of the galaxies, but in the absence of a robust method of positioning them in the $\log T_{\text{eff}} - \log g$ plane, the estimation for the intrinsic scatter should be taken with caution.

The zero point of the Cepheid period–luminosity relation is another issue for extensive debate. Conventionally, it is calibrated by assuming a distance modulus to LMC. However, since the quoted distance modulus to LMC ranges from less than 18.35 to more than 18.7 mag, we preferred to isolate the period–luminosity relation from this secondary calibration. Recent trigonometric parallax observations by the Hipparcos satellite (Feast & Catchpole

1997) provides us with direct distances to some of the nearby Cepheid variables. We have used the zero point calibration of this work and adopted the Hipparcos value of -4.24 for the mean absolute V -magnitude for a Cepheid of period 10 days. The same result is arrived at if we take only the three Cepheids of period > 10 days from their sample. Hence we have arrived at the following period–luminosity relation for Cepheid variables of period greater than 15 days:

$$M_V = -3.45 \log(P) - 0.79 \quad (1)$$

We assign a zero point error of 0.20 magnitude, though there is continuing debate on (a) whether Hipparcos parallax data systematically underestimates the distance to stars, and (b) whether the Feast and Catchpole (1997) calibration provides only an upper limit to the Cepheid distance scale.

4. Incompleteness Correction

A major task in the extragalactic distance measurement, like the HST observations of Cepheid variables in M100, is to isolate the signal from the noise near the limiting magnitude at which a precise determination of the stellar magnitude is barely feasible. We argued in Section 2 that the typical signal to noise ratio (SNR) for the HST observations of stars in M100 with filter F555W is around 6–8 for stars of V -magnitude near 26 and of the order of 10–15 for V -magnitude near 24.5. This rapid change in the SNR causes faint stars to be systematically missed in the sample, while the brighter stars preferentially detected at a fixed period produce an increase in the average brightness of the stars at that period, if the scatter in the period– V -magnitude diagram is large. (For instance, the HST data before extinction correction has scatter in the V -magnitude of order 0.45 magnitude at a fixed period). We now address the question: with this scatter in V -magnitude, is there a systematic over-estimation of the brightness of the M100 Cepheids at low periods? (i.e., is there the effect known as Malmquist bias (cf. Sandage 1987) in this sample?)

We can compare the HST sample of Cepheid variables in M100 with the reasonably complete sample of Galactic Cepheids (discussed in Paper I) to estimate this systematic effect. In Figure 2 we have displayed the observed number as a function of their period after carrying out a moving average for both the Galactic and M100 Cepheid variables. It is evident that almost all the HST data pertains to the Cepheids of period greater than 10 days, which lie in the second component of the Galactic distribution function (see Paper I). The ratio of the number density of the M100 Cepheids to that of the Milky Way is plotted as a function of the period in Figure 3, where we note the following features:

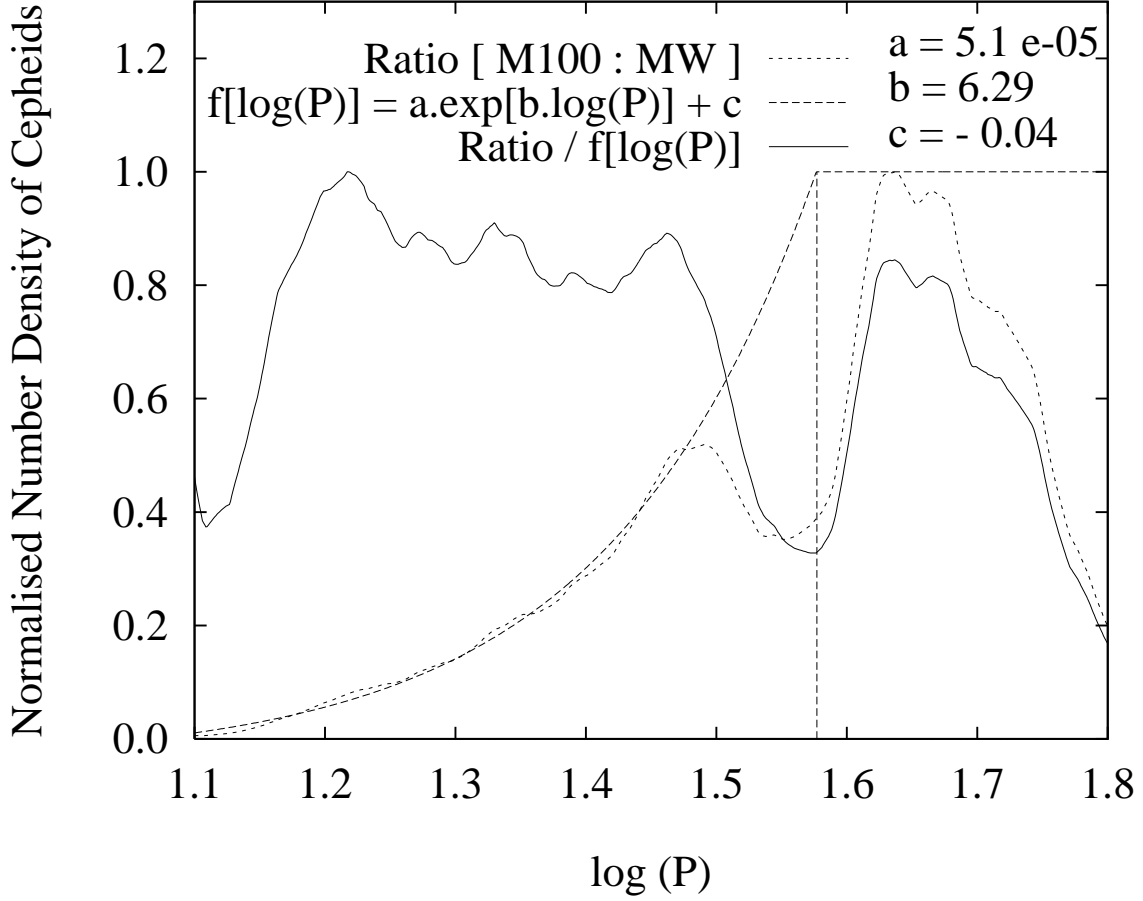


Fig. 3.— The ratio of number density distribution of Cepheids in M100 and the Galaxy is displayed (dotted curve). At low periods, an exponential curve $[5.1 \times 10^{-5} e^{6.29 \log(P)}] - 0.04$ is seen to fit this ratio well; when scaled by this function, the curve is seen to be free from flux-dependent incompleteness (solid curve).

- The ratio tends to a constant at large periods which is not surprising since the HST data has no systematic incompleteness at higher periods and also the galaxy M100 is similar to the Milky Way. But due to small number statistics of the Galactic sample, the shape of the graph is not reliable beyond a period around 50 days.
- At intermediate periods, there is a dip in the ratio indicating that most of the Cepheids at period of around 40 days have probably been missed. We argue later that this is owing to the fact that the HST data spans a duration of 57 days and observations were

carried out essentially at 11 epochs.

- At period lower than 30 days, the ratio between the number densities of M100 and Galactic Cepheids indeed shows a sharp decrease which we attribute to a systematic incompleteness due to the sample being flux-limited. The fall in the ratio with decreasing frequency is almost exponential, suggesting that the detection efficiency probably varies as some power of the number of photons received.

However, as we have demonstrated in Paper I, from the HST observations of Cepheids in galaxies at closer distances, the pattern of the HST distribution function appears to be similar to that of Galactic Cepheids, indicating that at magnitudes brighter than 22 mag, the effect is negligible.

The extent of incompleteness in the sample of M100 Cepheids is a combined effect of *(i)* magnitude-limited detection efficiency at low periods, *(ii)* intrinsic scatter in the period–luminosity relation, and *(iii)* increased scatter in the observed period– V -magnitude diagram due to errors in extinction correction as well as uncertainty in the determination of the pulsation period.

The detection of a signal as function of the number of data points and the signal to noise ratio was discussed in Section 2. If N_{ph} is the number of photons arriving at the telescope from a star, then it can be easily derived that the signal-to-noise ratio for bright objects is proportional to $\sqrt{N_{\text{ph}}}$, while for dim objects, it is proportional to N_{ph} itself. Thus, for sufficiently bright stars the probability of detection as a Cepheid with the HST scheme for M100 is practically a constant and the sample can be treated as though it was volume-limited. But for low period Cepheids the detection of pulsation with the 11 sample points becomes inefficient, although the observed efficiency would naturally depend on the algorithm used. Instead of going through these details, we can represent the detection efficiency for stars fainter than some cutoff magnitude V_0 by

$$D(V) \sim \exp[-\gamma(V - V_0)/\alpha], \quad (2)$$

where γ is a constant determined by the detector characteristics, α is the magnitude of the slope of the period– V -magnitude diagram, and V is the mean apparent magnitude of the star. The consequences of this for the distribution function of the Cepheids at a fixed period are discussed in the Appendix. At $V \gg V_0$, the incompleteness correction tends to a constant that depends only on the scatter in the period– V -magnitude diagram and the relation between SNR and efficiency of detection; this is because the stars mainly at the brighter end of the intrinsic distribution function at a fixed period are detected. At $V \ll V_0$, the correction tends to zero as to be expected.

As already noted in Section 2, the number density profile of M100 Cepheids shows a dip in the range $1.5 \leq \log(P) \leq 1.65$ caused due to the failure of detection of Cepheids. However, this decreased efficiency has no direct relevance to flux-limited incompleteness and we do not analyze it further. However, as we have discussed in the Appendix, the dip does introduce a systematic error when we try to determine the magnitude at which flux-limited incompleteness can be ignored, and consequently does affect the distance calibration.

If the probability density of the Cepheids as a function of the intrinsic magnitude retains its form and has the same scatter (σ) when the pulsation period varies, then any error in the determination of the period only increases the scatter in the observed period vs V -magnitude diagram. The error in the period can be incorporated in the observed probability density by replacing σ by an effective scatter (σ_{eff}) in the observed distribution, given by

$$\sigma_{\text{eff}} = [\sigma_{\text{int}}^2 + \frac{1}{6}\alpha^2\sigma_{\text{P}}^2]^{1/2} \quad (3)$$

correct to second order. Here σ_{int} is the intrinsic scatter in the period–luminosity diagram, while σ_{P} is the uncertainty in $\log(P)$. Based on our period determination methods, the value of σ_{P} is estimated to be around 0.1. For Cepheids with periods less than 30 days it is usually less than this value, while for $P > 30$ days, it lies between 0.1 and 0.2. For periods higher than 50 days, it is difficult to estimate the value of σ_{P} . If the extinction correction can be carried out in a manner independent of the incompleteness, σ_{eff} is the scatter in the period– V -magnitude diagram after the correction is applied. But in our scheme, we cannot carry out the correction independently of incompleteness as we use the period vs color, V -amplitude vs color-at-peak-brightness and the period– V -magnitude relations simultaneously. Consequently, the σ_{eff} we used is intermediate between the values in Figures 4 and 6.

We have carried out the correction for incompleteness bias as discussed in the Appendix, and our prescription to obtain a complete sample is

$$V_{\text{complete}} = \begin{cases} V_{\text{incomplete}} + \sigma_{\text{eff}}^2 \frac{\gamma}{\alpha} & \text{for } \log(P) \leq 1.52 \\ V_{\text{incomplete}} + \sigma_{\text{eff}}^2 \frac{\gamma}{\alpha} \frac{1.64 - \log(P)}{1.64 - 1.52} & \text{for } 1.52 < \log(P) \leq 1.64 \\ V_{\text{incomplete}} & \text{for } \log(P) > 1.64 \end{cases} \quad (4)$$

Within the observational errors this prescription agrees with the more detailed numerical results given in Table 3 based on the formulation described in the Appendix.

We should stress that this is a statistical method, where instead of increasing the mean magnitude at a fixed period by the specified correction term, we increase the magnitude of each star in that period range. The incompleteness-corrected V -magnitudes are shown along with the observed magnitudes in Figure 4. Note however, that the extinction-corrected $\langle V \rangle_0$ values in Table 1 are the *true* magnitudes for each star, not the incompleteness-corrected expectation value at the particular period.

Table 3: Incompleteness Correction based on Numerical Simulations

Cutoff Magnitude (V_0)	Effective Scatter (σ_{eff})	δV for period $\log(P)$				
		< 1.40	1.50	1.55	1.60	1.70
25.0	0.36	0.26	0.25	0.23	0.22	0.17
25.4	0.36	0.24	0.20	0.18	0.15	0.11
25.6	0.36	0.21	0.17	0.15	0.12	0.09
25.0	0.42	0.35	0.33	0.30	0.29	0.23
25.4	0.42	0.31	0.27	0.24	0.20	0.16
25.6	0.42	0.29	0.23	0.19	0.16	0.13
Value used in this work (from Figure 3)		0.28	0.28	0.21	0.09	0.00
Mean difference		0.00	-0.04	0.01	0.10	0.15

5. Extinction Correction

Extinction correction is important for distance calibration even for a face-on spiral like M100, since the stars observed at low periods would be predominantly of low extinction while at higher period the mean extinction is expected to be larger. In Paper I, we derived a formalism for the reddening and extinction correction for Galactic Cepheids, based on their multi-wavelength observations. However, in the absence of multi-color photometry or at least full light curves in two bands, the extinction correction carried out would be at most statistical in nature and would not take into account the differential extinction with respect to period. For want of better alternatives we have used the three relations, namely, $\langle V - I \rangle_0$ vs $\log(P)$, $(V - I)_0|_{\text{at } V_{\text{max}}}$ vs ΔV and $\langle V \rangle_0$ vs $\log(P)$, for distance calibration as well as extinction correction. However, we did not use pre-determined slope or intercept for any of these relations; instead, we resorted to L_1 minimization to obtain these six unknown quantities.

We prefer to use L_1 minimization over the standard practice of L_2 (χ^2) minimization for the following reason. The M100 data has large observational error bars, and since neither can we estimate the extinction well enough, nor can we identify the Cepheids in a different evolutionary stage (cf. Paper I), the scatter in the period–luminosity diagram as well as in the period–color–amplitude relations remains large. The L_2 minimization is much more sensitive to such noise in the data where the points having large error bars affect the mean values appreciably. Barrodale and Zala (1986) argue that L_1 is far more accurate in linear programming like ours where a few points far from the straight line should not contribute

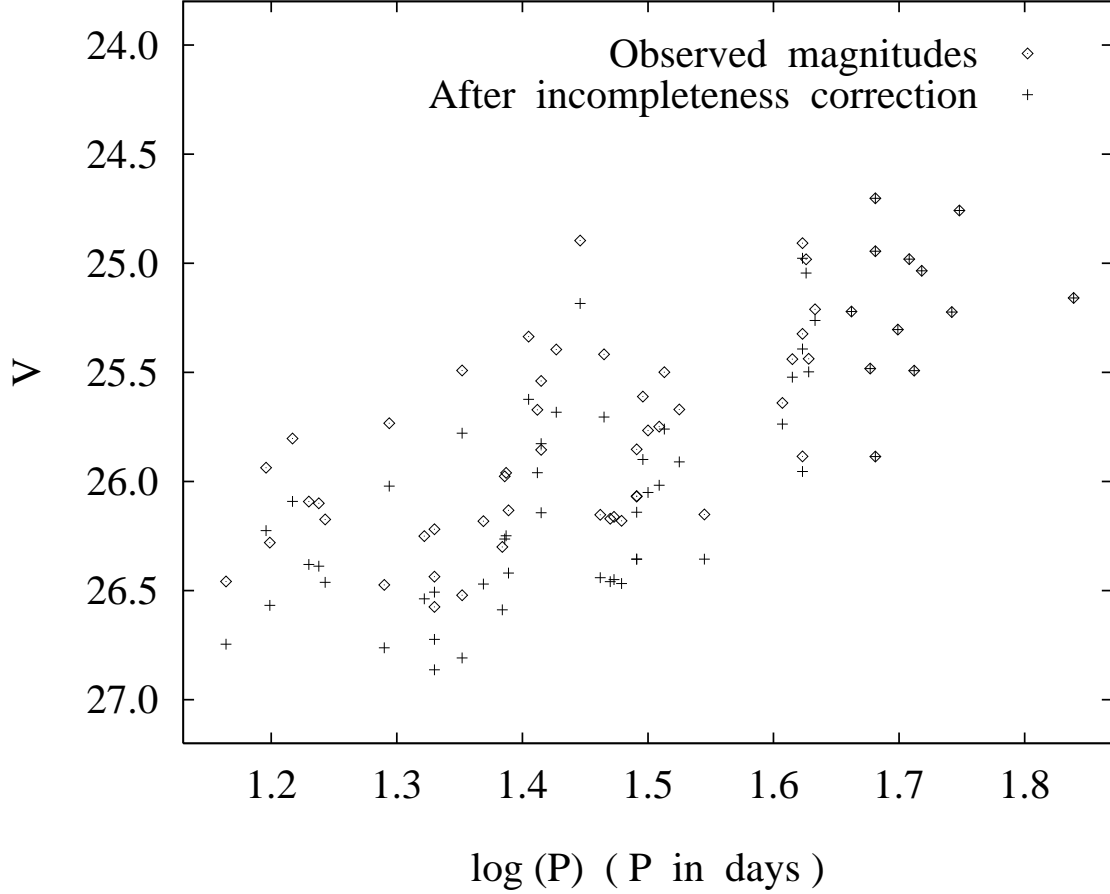


Fig. 4.— The raw V magnitudes of M100 Cepheids (obtained by integrating the light curves) and the statistically incompleteness-corrected magnitudes (according to Equation 4) are plotted against $\log(P)$.

substantially so as to change the slope or the intercept. The L_1 minimization leads to a value which is closer to the median of the sample, rather than the mean that would be expected from L_2 . Also, they argue that “trimming” is advisable for L_1 , which we have used only to distinguish between similar minima when we try a range of slopes and intercepts in the six-dimensional parameter space involving period vs $\langle V \rangle_0$, period vs $\langle V - I \rangle_0$ color and amplitude vs $(V - I)_0|_{\text{at } V_{\text{max}}}$ minimization.

We have adopted the linear relation between the reddening-corrected $\langle V - I \rangle_0$ and $\log(P)$, $(V - I)_0|_{\text{at } V_{\text{max}}}$ and ΔV as well as extinction and incompleteness bias corrected

$\langle V \rangle_0$ and $\log(P)$ for L_1 minimization. We minimize the absolute deviation χ_1 , defined by

$$\begin{aligned} \chi_1 = & \sum_i a_1 |\langle V \rangle_{0i} + \alpha \log(P_i) - \mu| + a_2 |\langle V - I \rangle_{0i} - \beta_1 \log(P_i) - y_1| \\ & + a_3 |\{(V - I)_0|_{\text{at } V_{\text{max}}}\}_i + \beta_2 \Delta V_i - y_2| \end{aligned} \quad (5)$$

Ideally the weights a_1 , a_2 and a_3 should be determined from the error estimates in the photometry as well as from the scatter in the three relations. We have chosen the three weights to be 0.2, 0.5 and 0.3 respectively in order that the scatter in both the best fit lines for $(V - I)$ are comparable to the errors in the observed colors in our data. The deviation χ_1 can be computed for a specified set of parameters α , β_1 , β_2 , μ , y_1 and y_2 by choosing the reddening $E(V - I)$ and extinction A_V for each star. We have chosen a constant ratio $A_V/E(V - I) = 2.44$ in the absence of multi-band observations (see e.g., Cardelli, Clayton & Mathis 1989). The mean dereddened color and its value at the brightest phase are both taken to be $\langle V - I \rangle_0 = \langle V - I \rangle - E(V - I)$ and $(V - I)_0|_{\text{at } V_{\text{max}}} = (V - I)|_{\text{at } V_{\text{max}}} - E(V - I)$.

For each data point the minimum deviation will be produced either at zero extinction or when the point falls on one of the three straight lines, subject to $E(V - I) > 0$. The minimization of χ_1 with respect to the intercept μ in the period– V -magnitude relation provides the estimate for the distance modulus if the other parameters are fixed. The respective slopes β_1 and β_2 for the Galactic Cepheids were found to be 0.13 and 0.28 (cf. Paper I) and in Section 3 we argued that $\alpha \sim 3.45$. But since the statistics for the Galactic sample is not very robust, we kept the two intercepts for the color diagram as well as all the three slopes to be unknowns having narrow range of acceptable values. For the period– V -magnitude relation we scanned for slopes between -3.30 to -3.60 to obtain a value of -3.49 , though for higher incompleteness correction at certain periods a slope of -3.52 and a higher intercept would be preferred. Similarly, our χ_1 -minimized values $\beta_1 = 0.13$ and $\beta_2 = 0.30$ match with the Galactic values within 0.02. However, the intercepts, $y_1 = 0.69$ and $y_2 = 0.94$ show a difference of 0.02 and 0.05 respectively, but in view of the corrections not included (which we discuss below), we consider the intercepts to be consistent with their Galactic counterparts. This agreement in spite of substantial error in the individual $\langle V - I \rangle$ values makes us trust the final distance modulus to at least within the errors we have given. The average extinction, A_V is 0.30 mag which agrees with the results of other workers but in view of the Malmquist bias of 0.28 mag at low periods, a value of $\langle A_V \rangle \approx 0.20$ – 0.25 would have been comfortable.

It should be noted that many of the points lie exactly on the lines in the three plots (Figures 6 and 7); this is a natural consequence of the L_1 minimization where the expectation value is closer to the median than to the mean. We shall like to again stress that the procedure automatically assigns less weightage to the few data points far from the line either due to large errors or due to the star being at a different stage of evolution.

The following effects could not be studied quantitatively and hence their contribution to the error in the distance modulus cannot be ascertained:

The four fields of M100 where Cepheids were observed will contain numerous unresolved red dwarfs. Their presence is unlikely to change the V -magnitude of the Cepheids but they could modify the $(V - I)$ light curve, though the variation will depend upon the method employed to subtract the background. This will affect the extinction correction as well as possible tests on metallicity of the Cepheids in M100, but in the absence of reliable I band light curve we cannot carry out quantitative analysis of this effect.

The Galactic Cepheids which are not at the second passage of the instability strip follow different period–color–amplitude relations. It was shown in Paper I that their presence in the sample can increase the slope of the $\langle B - V \rangle_0$ vs $\log(P)$ relation from ~ 0.2 to nearly 0.4 and that they are detectable from their conspicuously different positions on the $\log T_{\text{eff}} - \log g$ plane. However, for the M100 Cepheids with only sparsely sampled observations in two bands, neither the position of the instability strip on the $\log T_{\text{eff}} - \log g$ plane can be determined, nor can the pulsators at different evolutionary stages be identified. The contamination from stars at first or third passage of the strip will introduce errors in the final period–color–amplitude and period–luminosity relations of M100 Cepheids.

The Galactic Cepheids of period larger than 15 days have an average V band pulsation amplitude of ~ 1.1 mag and most of these variables have amplitude greater than 0.8 mag. But from Figure 5, it is evident that the M100 Cepheids in the same range of period have V -amplitudes generally lower than their Galactic counterparts, the reason for which is not known. Moreover, the amplitude appears to decrease on the average, when the period of pulsation increases. Both these effects could be an artifact of the sparse sampling or due to observations of specific regions in M100, unlike the Galactic sample which is not confined to any part of the Milky Way. Nevertheless, the amplitude vs color-at-maximum relation should be scrutinized to examine whether we compare similar samples in two different galaxies.

6. Results and Discussion

The final result for the Cepheid variables in the spiral M100 in Virgo Cluster, after corrections for extinction and incompleteness of the sample and after carrying out the L_1 minimization, is given by the period– V -magnitude relation (Figure 6)

$$\langle V \rangle_0 = -3.49 \log(P) + 30.80, \quad (6)$$

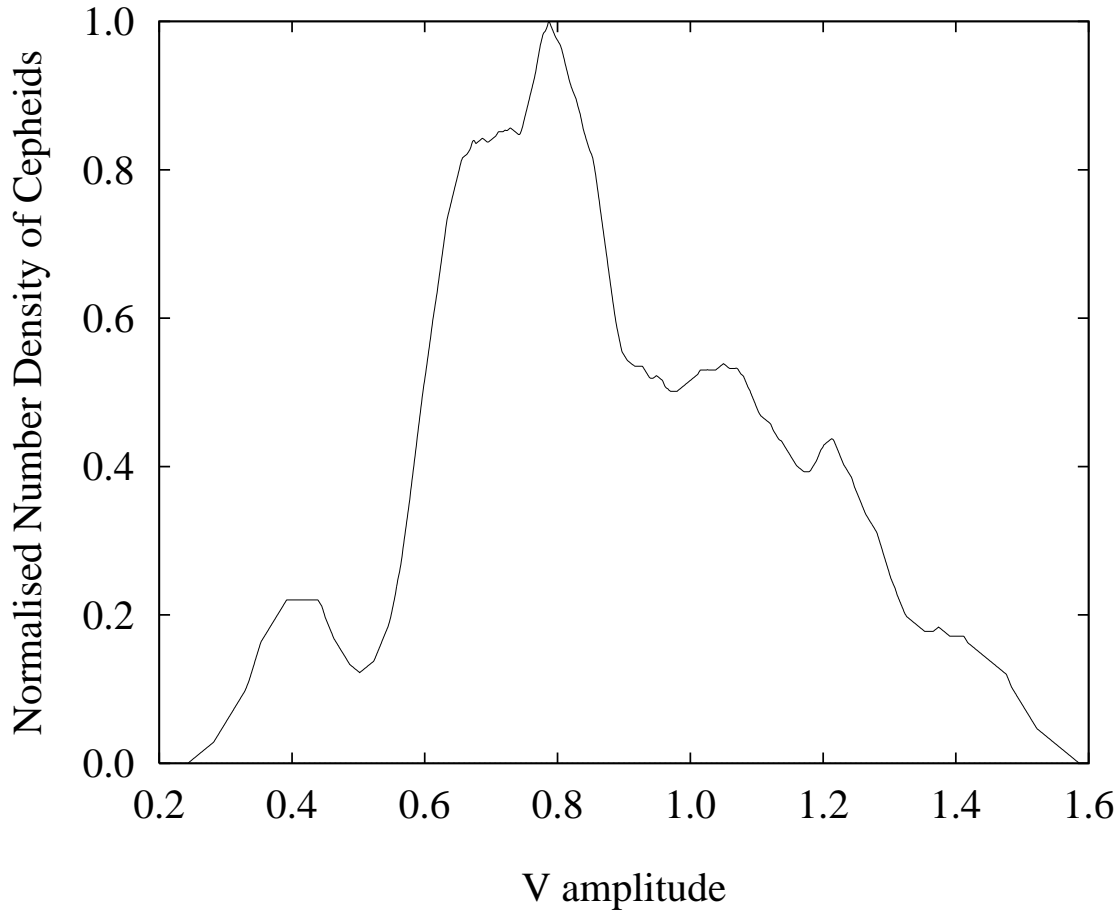


Fig. 5.— The normalized number density of M100 Cepheids as a function of their V amplitudes of pulsation are shown. A moving average has been used to generate a smooth curve from discrete observations.

the period–color relation (Figure 7)

$$\langle V - I \rangle_0 = 0.13 \log(P) + 0.69, \quad (7)$$

and the V -amplitude–color-at-brightest-phase relation (Figure 7)

$$(V - I)_0|_{\text{at } V_{\text{max}}} = -0.30\Delta V + 0.94 \quad (8)$$

If the period–color–amplitude–luminosity relation for the Galactic Cepheids had been better established and the I band light curve of the Cepheids in M100 were observationally determined, the minimization would have been possible with fewer unknown parameters.

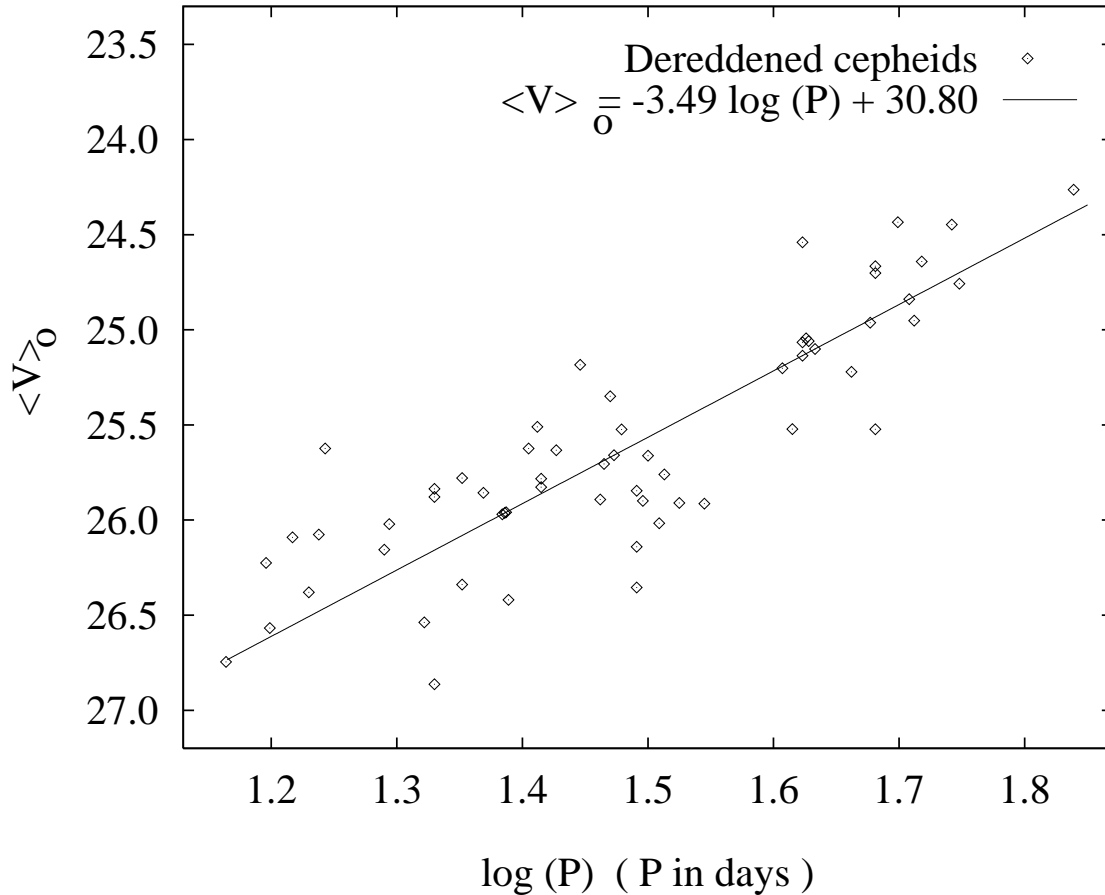


Fig. 6.— The final PL diagram for M100 Cepheids is shown, along with the plot for the best fit period–luminosity relation.

This would have provided better tests of the result as well as of the internal consistency of the data. The specific issue is: does the sample observed in M100 belong to the same population to which the Galactic Cepheids belong to, or are the Galactic Cepheids studied so far subject to systematic biases? Similarly, if the errors in the period determination were fewer, there would have been less mixing in the observed period– V -magnitude diagram and the scatter in the diagram could have been considerably less at periods in the range of 35 to 45 days, which is the crucial region in determining the distance modulus. At present, the error estimates should be treated as indicative only, since we do not have sufficient internal checks on them.

Here we discuss some of the additional problems which, we feel, should be addressed

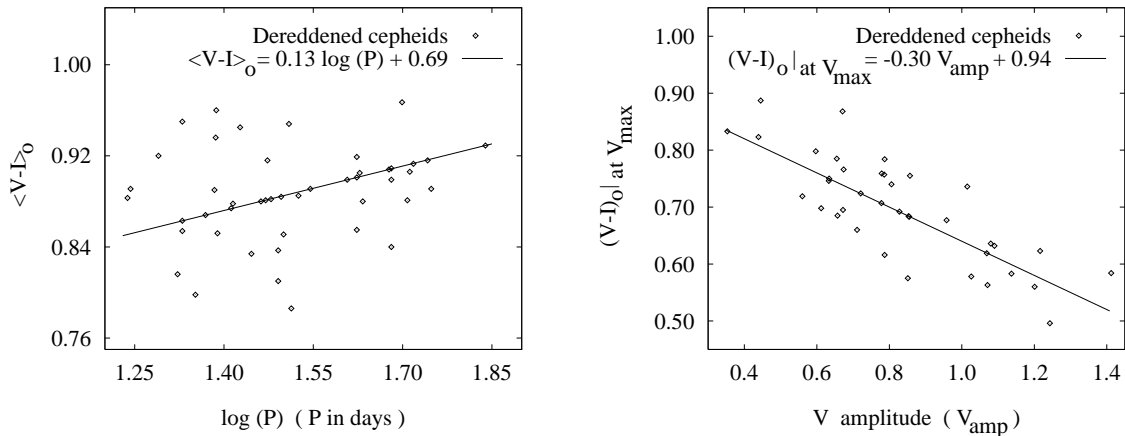


Fig. 7.— Period–color and amplitude–color plots for the M100 Cepheids are shown along with the best fit linear relations.

adequately in future key projects:

The mean extinction correction is only as reliable as the colors even if the period is known accurately. We estimate that the $(V - I)$ data has approximately 0.15 magnitude error. Since the average reddening is of the order of 0.10 and probably much less for the variables of low period, many of the Cepheids show negative reddening. In our treatment, these stars would have zero extinction and this systematically overestimates the mean extinction. When the Malmquist bias for Cepheids fainter than 25.2 magnitude is taken into account for the present M100 sample, we find that half the Cepheids are susceptible to this error at period of less than 40 days. This was also borne out by our analysis. Should our estimation of the cutoff magnitude for flux-limited bias of 25.2 magnitude be correct, we might be overestimating the extinction by approximately 0.1 magnitude and ultimately the distance to M100 by the same amount.

In Figure 3 we were unable to determine the shape of the curve (relative number density of Cepheids in M100 to that in the Milky Way, as function of the pulsation period) at 35 to 45 days because of the dip in the number density of Cepheids detected in M100 due to extraneous reasons. This has indirect implications for the correction to the flux-limited detection efficiency as is discussed in the Appendix and it could possibly explain some skewness in Figure 6.

Within these limitations, the resulting period– V -magnitude relation for the Cepheids in M100 can be compared with the one we have arrived at in Section 3 to determine the distance modulus to M100 to be 31.55 mag, i.e., a distance of 20.42 Mpc. Our main results

as well as the error contributions from various sources that were analyzed are summarized in Table 4. The random error is computed by finding the change in the intercept μ when χ_1 is increased by half the maximum deviation from the best fit line after neglecting the three worst points.

Thus, our estimation of the distance to M100 is 20.42 ± 1.7 (random) ± 2.4 (systematic) Mpc. Taking into account the position of M100 relative to the center of Virgo Cluster, the distance to the Virgo Center is estimated to be 20.42 ± 1.7 (random) ± 2.6 (systematic) Mpc.

The present work does not address the problem of recession velocity of the Virgo Center with respect to the Local Group. We would however, point out that if one takes a central line-of-sight velocity dispersion, σ_V , of the order of 800 km s^{-1} and structural length, a of 1.5 Mpc for the Virgo Cluster, the velocity of the Local Group towards Virgo produced by the mass centered at Virgo Cluster would be of the order of

$$V_{\text{peculiar}} \sim \frac{3\sigma_V^2 a}{R^2} \tau \sim 75 \text{ km s}^{-1} \quad (9)$$

where R is the distance to Virgo Center and τ is the age since the formation of Virgo Cluster. Rowan-Robinson (1988) argued that from the IRAS data there is no evidence for appreciable Virgo-centric flow which is consistent with our simplistic calculation. We take the recession velocity of Virgo to be $1170 \pm 80 \text{ km s}^{-1}$ (cf. Jerjen & Tammann 1993) and estimate the Hubble Constant to be

$$H_0 = 57 \pm 5 \text{ (random)} \pm 8 \text{ (systematic)} \text{ km s}^{-1} \text{ Mpc}^{-1} \quad (10)$$

7. Summary and Prospects

Our strategy to investigate the calibration of Cepheids based on extragalactic distance scale is two-fold:

- Preparation of a reasonably well tested local complete sample of the parent population of Cepheid variables and quantification of some of their characteristics for using them as benchmarks for a determination of distance to far off galaxies.
- Carrying out tests on a set of homogeneous data of good quality for the external galaxy and devise a method to extract the calibration characteristics without getting unduly distorted by the noise.

Table 4: Results and Error Budget

Quantity	Unit	Mean Value	Random Error	Systematic Error	Comments
Calibration of the Period-Luminosity relation:					
Slope		−3.45		0.08	No good test sample.
Intercept	mag	−0.79		0.20	Distance to nearby Cepheids. Extinction correction.
Period- V -magnitude relation for M100:					
Slope		−3.49			Some Cepheids of $P > 55$ days could appear at 48–55 days.
Intercept	mag	30.80	0.10	0.10	Extinction and incompleteness corrections not independent.
Extinction correction	mag	0.30	0.08	0.08	Error in $(V - I)$ large Reddening due to unresolved stars. Recession of M100 — K correction. Galactic period-color-amplitude relations not well-determined.
Incompleteness correction	mag	0.28	0.12		Model for the efficiency of detection not known. Error in periods.
Zero point calibration of the detector	mag			0.08	Observational problem.
Distance modulus to M100	mag	31.55	0.18	0.26	
Distance to M100	Mpc	20.42	1.7	2.4	
Distance to Virgo	Mpc	20.42	1.7	2.6	Position of M100 with respect to Virgo center.
Recession velocity of Virgo	km/s	1170		80	Infall to Virgo Center of Local Group not same as velocity component towards Virgo.
Hubble Constant	km/s/Mpc	57	5	8	

For the Galactic Cepheid variables, we were guided by the light curves, number density as function of period and amplitude, and by the theory of stellar pulsation. Our attempts to determine the position of Galactic Cepheids in the *surface temperature–surface gravity plane* was not very successful: we are not very confident with our comparison of the theoretical colors with the observed values because the presently available model atmospheric ($U - B$) calibration appears to need better input physics. The models based on stellar pulsation are

limited by the size of the helium core, and the boundary conditions in the outer envelope where convection is supersonic, apart from the more fundamental problem of coupling between convection and pulsation. Still, as a working model, the $\log T_{\text{eff}} - \log g$ strip we have determined and the period–color–amplitude relations we obtained should be useful for the calibration of the Cepheid distance scale.

We used HST data on Cepheids for galaxies at distance modulus of the order to 28 to 29 magnitudes to determine the slope of the period– V -magnitude relation for the population that would be targeted for the measurement of distances to farther galaxies. The slope of the relation appears to be consistent between various galaxies. Equally important is the intrinsic scatter in the relation if we wish to provide a trustworthy error analysis of our distance estimations, but we do not have good enough data yet to determine the extinction corrected scatter. We have discussed the implications of this drawback.

We have used L_1 minimization for the determination of distance modulus of M100. We have attempted a correction for flux-limited incompleteness by using a diagram of the relative number density of Cepheids in M100 as function of the period. We also carried out numerical simulations using a toy model for the distribution function of the population and the efficiency of the detector. We provide a prescription for correction to offset the flux-limited incompleteness in a sample when a volume-limited test sample of the same population is available.

It is indicated from our analysis that a reliable estimate of the distance to galaxies situated within 40 Mpc is well within the capability of the HST provided the observing strategy addresses some of the problems specific to Cepheids which we have attempted to highlight in the present work. But it should also be realized that a systematic error of approximately 0.25 magnitude should be eliminated by observing a selected sample of local Cepheid variables.

We are grateful to W. Freedman for sending the LMC data of Cepheid variables and to L. Ferrarese for sending a draft of their work on the HST key project on Cepheids in M100. We are thankful to S.M.Chitre for many helpful comments on the manuscript. We acknowledge support from the Indo-French Center for the Promotion of Advanced Research (Project 1410-2).

APPENDIX

A. Incompleteness Correction: Mathematical Formulation and discussion of certain Systematics

The astrophysical data is very often prone to incompleteness due to limitation in the flux of radiation received from the source, thereby systematically favoring detection of the brighter of the objects having otherwise nearly identical properties. This effect, known as Malmquist bias, has been discussed extensively in the literature (e.g. Sandage 1987). Even though theoretically this effect is pretty well understood, its quantification is nontrivial because the local volume-limited sample is usually subject to large random and systematic errors due to small number statistics or specific environment effects, though it is not limited by the faintness of the objects. Thus, for example, the local environments of Cepheid variables in our neighborhood may be different from that of a distant galaxy we are observing and hence the local sample may not represent the parent population to be analyzed or there may be too few stars within some range of period in our complete sample causing the random noise to overwhelm the properties we intend to characterize. Consequently, researchers are rarely in agreement on whether a given set of data is biased due to flux limitation or whether a correction needs to be applied to offset the Malmquist bias. In this section, we try to use a simple mathematical model to estimate the effect and later provide an alternative easy-to-implement way using a diagram which can be drawn with the available data, provided the observations of the local sample and of the distant objects are carried out with a few precautions. By comparing these results, we give a prescription for the quantification of Malmquist bias in a sample, with the Cepheid population as a specific example.

For the sake of tractability and ease of interpretation, we analyze a simple model for the unnormalized probability density as a function of the V -magnitude for a constant period of the Cepheid variables, of the form

$$f(V, P_{\text{tr}}) = N(P_{\text{tr}}) \exp \left[-\frac{\{V - \mu + \alpha P_{\text{tr}}\}^2}{2\sigma^2} \right], \quad (\text{A1})$$

where V is the extinction corrected mean V -magnitude of the star, P_{tr} is $\log(P)$ of pulsation if there were no error in the estimation of the period, μ is the zero point of the Cepheid period– V -magnitude relation for the galaxy, α the negative of the slope, and σ the intrinsic scatter in the relation. The expression for the normalization term $N(P_{\text{tr}})$ in the probability density could have explicit dependency on period as well as V -magnitude, but ours seemed to be a reasonable approximation. The distribution of Cepheid variables within the instability strip is far from Gaussian, but that deviation will only increase the incompleteness

and consequently, in our first attempt to study this systematic effect we will not be over-estimating the correction if we use the Gaussian form. The errors in the observed period is a major handicap, specifically to estimate the magnitude at which the incompleteness becomes important. But we take the simplistic view that the probability density can be expressed as a function of the observed period by suitably weighted integration of the above expression over period, and that the only change due to the integration is an increase in the scatter σ as argued in Section 4. Further, depending upon whether extinction correction is carried out independent of the incompleteness correction or not, the value of an effective σ_{eff} will be defined to incorporate the scatter in the observed period vs V -magnitude diagram after the extinction correction is over. We make the working hypothesis that the efficiency of the detector to find a Cepheid variable depends only on the apparent magnitude of the star, V_a , and consequently we can analyze the incompleteness correction at a fixed period of pulsation. Accordingly, we assume that the efficiency of detection, $D(V_a)$ is given by

$$D(V_a) = \begin{cases} 1 & \text{if } V_a \leq V_0 \\ \exp[-\gamma(V_0 - V_a)/\alpha] & \text{if } V_a > V_0 \end{cases} \quad (\text{A2})$$

where V_0 is the cut off magnitude below which there is no incompleteness of the sample due to flux limitation.

On account of flux limitation, the distribution function at the observed period $P_0 \equiv \log(P/\text{day})$ becomes

$$f_0(V_a, P_0) = f(V, P_0) D(V_a) \quad (\text{A3})$$

We assume that subject to detectability, all extinction values > 0 are allowed. Hence, integrating over the extinction, $\epsilon = V_a - V$ from 0 to ∞ at equal weight, we get the probability density within a normalization constant, as

$$\Theta(V, P_0) = \begin{cases} [1 + \gamma(V_0 - V)/\alpha] f(V, P_0) & \text{if } V \leq V_0 \\ \exp[\gamma(V_0 - V)/\alpha] f(V, P_0) & \text{if } V > V_0 \end{cases} \quad (\text{A4})$$

The probability density can thus be written as

$$F_{\text{obs}}(V, P_0) = \frac{\Theta(V, P_0)}{\int \Theta(V, P_0) dV} \quad (\text{A5})$$

If there is no incompleteness, the expectation value of $(V - \mu + \alpha P_0)$ will be zero. The flux limitation decreases the value and this decrement is a measure of the incompleteness correction.

When $(\mu - \alpha P) \ll V_0$, the incompleteness will be negligible and if $(\mu - \alpha P - V_0) > 2\sigma_{\text{eff}}$, the incompleteness will tend to a constant value ($= \gamma\sigma_{\text{eff}}^2/\alpha$). Results from this model calculations for various values of V_0 and σ_{eff} are given in Table 3.

The various simplistic approximations used render the error analysis rather difficult. But most of the difficulties could be resolved if we use the observed data of the complete sample of local Cepheids and the stars in the external galaxy. The incompleteness could be reliably estimated by resorting to the equivalent of Figure 3 with the V -magnitude as the abscissa, if the ratio of the number density as a function of V -magnitude (i.e. the variable determining the incompleteness) had been available. In the absence of such a plot, the period of pulsation is converted into an equivalent V -magnitude and used for the incompleteness correction through Figure 3. If indeed we can use the V -magnitude as abscissa, the measure of incompleteness at a specified period of pulsation is simply the *scatter in the V -magnitude for a fixed period*, σ_{eff} , *times the decrease in the logarithm of the ratio of the number density in the observed sample to the number density in the complete sample when the abscissa is increased by an amount σ_{eff}* . Since these quantities can be plotted without any detailed modeling like we have shown in Figure 3, we can carry out the extinction correction as well as possible error analysis in our estimate according to the approximate prescription given in Section 4 and the numerical values are shown in Table 3. But it should be stressed that, though the dip in the observed number density of Cepheids in M100 at period of 35 to 45 days due to detection strategy does not directly introduce incompleteness corrections, it makes it difficult to determine the cutoff magnitude V_0 beyond which there is flux-limited incompleteness. Consequently, the peak of the flat region in Figure 3 as well as the period at which the peak is attained are uncertain. This is the region where our approximation based on Figure 3 and the numerical simulations differ considerably as we see in Table 3, but since both the methods are subject to systematic errors introduced because of the distortion in the figure, we do not feel either of the method is superior.

REFERENCES

- Barrodale, I. & Zala, C. 1986, in Numerical Algorithms, ed. J. L. Mohamed & J. E. Walsh (Clarendon Press, Oxford), 220
- Bhat, M., Gandhi, B., & Narasimha, D. 1998, work in progress
- Cardelli, J. A., Clayton, G. C., & Mathis, J. S. 1989, ApJ, 345, 245
- Feast, M. W., & Catchpole, R. M. 1997, MNRAS, 286, L1
- Ferrarese, L., et al. 1996, ApJ, 464, 568
- Freedman, W. L., et al. 1994, Nature, 371, 757
- Freedman, W. L. 1995, private communication

- Freedman, W. L., Mould, J. R., Kennicutt, R. C., Madore, B. F. 1998, in IAU Symposium No. 183, *Cosmological Parameters and the Evolution of the Universe*, ed. K. Sato, in preparation (astro-ph/9801080)
- Graham, J. A., et al. 1997, *ApJ*, 477, 535
- Horne, J. H., & Baliunas, S. L. 1986, *ApJ*, 302, 757
- Jerjen, H., & Tammann, G. A. 1993, *A&A*, 276, 1
- Morgan, S. 1994, *ASP Conference Series*, Vol. 57, 145
- Press, W. H., & Rybicki, G. B. 1989, *ApJ*, 338, 277
- Rowan-Robinson, M. 1988, *Space Sci. Rev.*, 48, 1
- Saha, A., & Hoessel, J. G. 1990, *AJ*, 99, 97
- Saha, A., Labhardt, L., Schwengeler, H., Macchetto, F. D., Panagia, N., Sandage, A., Tammann, G. A. 1994, *ApJ*, 425, 14
- Saha, A., Sandage, A., Labhardt, L., Tammann, G. A., Macchetto, F. D., Panagia, N. 1996, *ApJ*, 466, 55
- Sandage, A. 1987, in IAU Symposium No. 124, *Observational Cosmology*, ed. A. Hewitt, G. Burbidge, & L. Z. Fang, 1
- Sandage, A., Saha, A., Tammann, G. A., Labhardt, L., Schwengeler, H., Panagia, N., Macchetto, F. D. 1994, *ApJ*, 423, L13
- Silbermann, N. A., et al. 1996, *ApJ*, 470, 1